Food Chemistry: X 23 (2024) 101756

Contents lists available at ScienceDirect

Food Chemistry: X

journal homepage: www.sciencedirect.com/journal/food-chemistry-x

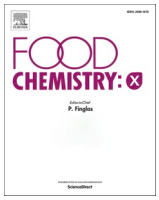

Improvement in probiotic intestinal survival by electrospun milk fat globule membrane-pullulan nanofibers: Fabrication and structural characterization

Yucong Wang [a,1], Zhixin Xie [a,1], Haitian Li [a], Gongsheng Zhang [a], Rongxu Liu [b], Jianchun Han [a,b,*], Lili Zhang [a,**]

[a] College of Food Science, Northeast Agricultural University, Harbin 150030, China
[b] Heilongjiang Green Food Science Research Institute, Harbin 150030, China

ARTICLE INFO

Keywords:
Milk fat globule membrane
Pullulan
Whey protein isolate
Electrospun fibers
Encapsulation
Probiotics

ABSTRACT

Studies have demonstrated the protective effect of milk fat globule membrane (MFGM) on probiotics in harsh environments. However, currently, there are no reports on the encapsulation of probiotics using MFGM. In this study, MFGM and pullulan (PUL) polysaccharide fibers were prepared by electrostatic spinning and used to encapsulate probiotics, with whey protein isolates (WPI)/PUL as the control. The morphology, physical properties, mechanical properties, survival, and stability of the encapsulated *Lacticaseibacillus rhamnosus* GG (LGG) were studied. The results showed that the MFGM/PUL solution had significant effects on pH, viscosity, conductivity, and stability. Electrostatic spinning improved the mechanical properties and encapsulation ability of the polymer formed by MFGM/PUL. LGG encapsulated in MFGM/PUL nanofibers survived rate was higher than WPI/PUL nanofibers in mimic intestinal juice, which could be attributed to the phospholipid content contained in MFGM. These results demonstrate that MFGM is a promising material for probiotic encapsulation, providing an important basis for the potential use of MFGM/PUL nanofibers as a robust encapsulation matrix.

1. Introduction

The growing emphasis on health has stimulated the demand for food safety and beneficial health attributes. Probiotics have emerged as a focal point in the functional foods field, with demonstrated the ability to regulate gastrointestinal microbiota, enhance immunity, and promote gut health (Salminen et al., 2021). However, probiotics inevitably face challenges from gastric acids, hydrolytic enzymes, bile salts, and other environmental factors as they pass through the gastrointestinal tract. These combined factors result in the death of a significant numbers of probiotics and prevent their ability to colonize the intestinal epithelium, consequently impeding their efficacy (Chou & Weimer, 1999; Liu et al., 2007). To overcome this problem, researchers have employed encapsulation technologies to protect probiotics. This ingenious approach succeeds in moderating the interaction between probiotics and the external environment to a certain extent, thereby preserving the bacterial architecture and biological vitality. Encapsulation not only protects probiotics from harmful influences, but also offers the prospect of enhancing their functionality (Martín, Lara-Villoslada, Ruiz, & Morales, 2015). Therefore, the search for a suitable encapsulation method specific to probiotics, coupled with the identification of an encapsulation material matrix with robust stability, is of profound significance.

Probiotics encapsulation is primarily achieved by entrapping both protective agents and microorganisms within emulsions. This process results in the formation of composite particles or fibers. Various techniques, including spray drying, gelation, co-precipitation, and electrospinning, can be employed to prepare these composites (Chang, Lambo, Liu, & Li, 2021; Frakolaki, Giannou, & Tzia, 2023; Paéz et al., 2012). In contrast to traditional encapsulation techniques, such as lyophilization, spray drying, and microencapsulation, electrospinning technology is a novel approach for probiotic encapsulation. Electrospinning offers multiple advantages, including increased production efficiency, simple

* Corresponding author at: Key Laboratory of Dairy Science, Ministry of Education, College of Food Science, Northeast Agricultural University, Harbin 150030, China.
** Corresponding author.
E-mail addresses: hanjianchun@hotmail.com (J. Han), lilizhang2011@163.com (L. Zhang).
[1] Equal contribution.

https://doi.org/10.1016/j.fochx.2024.101756
Received 3 June 2024; Received in revised form 17 August 2024; Accepted 19 August 2024
Available online 22 August 2024
2590-1575/© 2024 The Authors. Published by Elsevier Ltd. This is an open access article under the CC BY-NC-ND license (http://creativecommons.org/licenses/by-nc-nd/4.0/).

operation, mild processing conditions, and cost-effectiveness (Librán, Castro, & Lagaron, 2017). This advanced technology ensures the precise embedding and efficient delivery of probiotics, simultaneously improving their survival rate and stability (Ma et al., 2021). In addition, the high porosity and specific surface area of nanofibrous membranes provide superior protection and release efficiency for probiotic encapsulation. Its mild preparation conditions help to maintain probiotic activity, and the size and morphology of the nanofibrous membrane film can be precisely tuned, facilitating the tailoring of probiotic release characteristics (Chang et al., 2021; John et al., 2022; Xu, Ban, Wang, Hou, & Jiang, 2022). Therefore, the preparation of nanofibrous membranes by electrostatic spinning represents a groundbreaking method for probiotic encapsulation, offering broad application potential and significant research value.

Pullulan (PUL) is an extracellular, water-soluble polysaccharide, characterized as a tasteless, odorless, colorless, non-crystalline powder. Its remarkable properties include high water solubility and consistent solution viscosity (Jia et al., 2020). PUL has been found to be widely useful demonstrated high utility in electrospinning and as a spinning auxiliary material owing to its exceptional film-forming ability and the ability to generate fibers or films with impressive oxygen barrier properties and degradability (Drosou, Krokida, & Biliaderis, 2018). A previous study confirmed that PUL and whey protein isolate (WPI) blends could electrostatically produce nanofibers, suggesting that PUL and WPI can be employed in electrospinning and as spinning aids (Ali, Jiang, Chen, Ashraf, & Tahir, 2023).

Milk fat globule membrane (MFGM) is a three-layer membrane structure tightly wound around the surface of encapsulated milk fat droplets. In recent years, liposomes derived from MFGM and its derivatives have been widely used, especially for the encapsulation of bioactive compounds such as curcumin, lactoferrin, ascorbic acid, and tea polyphenols (Farhang, Kakuda, & Corredig, 2012). Numerous studies have demonstrated a symbiotic association between *Lacticaseibacillus* and milk matrix components, underscoring their potential to enhance the efficacy of bacterial entrapment and targeted release in the intestinal environment. The interaction between MFGM glycoproteins and probiotics is of particular note. This synergy enhances bacterial positioning within microparticles, strengthens their resilience to the gastric environment, and facilitates their journey to specific destinations while preserving their vitality (Gallier, Tolenaars, & Prosser, 2020; Guerin, Burgain, Gomand, Scher, & Gaiani, 2019). Based on these findings, MFGM appears to be an innovative and promising vehicle for probiotics encapsulation.

Studies have established the protective effect of MFGM on *Lacticaseibacillus rhamnosus* GG (LGG) against bile stress (Zhang et al., 2020). However, there are gaps in the literature regarding the preparation of nanofibers for encapsulating probiotics via electrospinning using a mixed solution of MFGM and PUL. As electrospun nanofibers for food packaging must be biocompatible and process low toxicity, we chose MFGM and WPI as encapsulation materials. In this study, the optimal solution ratio of MFGM/PUL nanofibers was determined using WPI/PUL as the control, and the structural features of MFGM/PUL nanofibers were analyzed using different characterization methods, namely scanning electron microscopy (SEM), attenuated total reflection-Fourier transform infrared spectroscopy, X-ray diffraction, thermogravimetric analysis (TGA), and mechanical properties. The distribution of LGG encapsulated in MFGM/PUL nanofibers was observed using SEM and fluorescence microscopy. Changes in viability, storage stability, and tolerance to gastrointestinal fluids and bile salts after LGG encapsulation in MFGM/PUL nanofibers were also examined. The aim of these experiments was to evaluate the potential application of MFGM/PUL nanofibers for lactic acid bacteria encapsulation and to provide a theoretical and experimental basis for novel lactic acid bacteria encapsulation materials.

2. Materials and methods

2.1. Bacterium and growth condition

Lacticaseibacillus rhamnosus GG (LGG) (CICC 6141) was purchased from China Industrial Culture Collection Center (Beijing, China). LGG preserved in 25% (*v*/v) glycerol was removed from the ultra-low temperature refrigerator (−80 °C) and inoculated in de Man, Rogosa, and Sharpe broth (Aoboxing Biotechnology Co., Ltd., Beijing, China, 1%, v/v) at 37 °C overnight. The above incubation steps were repeated thrice times to increase the viability of the LGG strain for future experiments.

2.2. Preparing electrospun nanofibers

The polymer solution was prepared according to a previously describes method with minor modifications (Ma et al., 2021). MFGM-10 (MFGM, Arla Food Ingredients, Aarhus, Denmark), whey protein isolate 90 (WPI, Hilmar Ingredients, Texas, USA), and pullulan (PUL, Baichuan Biotechnology Co., Ltd., Tianjin, China) were dissolved in distilled water to obtain a 20% (*w/v*) solution. Solutions of MFGM: PUL and WPI: PUL were prepared at various weight ratios (100:0, 80:20, 70:30, 60:40, 50:50, 40:60, 30:70, 20:80 and 0:100) and magnetically stirred (RET B S25, IKA, Germany) at 500 rpm for 6 h at room temperature to promote sufficient dissolution of the polymer materials.

The electrospinning process was performed according to a previous study (Jia et al., 2020) using an electrospinning device (TEADFS-700, Technova Technology Co., Ltd., Beijing, China) with a high-voltage DC power supply, syringe, and grounded aluminum foil collector. The polymer solution was introduced into a 10 mL syringe. A voltage of 20 kV was applied between the syringe needle and a grounded aluminum foil collector. The solution was dispensed at a controlled flow rate of 0.8 mL/h, while the distance between the needle and the collector was maintained at 15 cm. Electrospinning temperature and relative humidity were controlled at 25 °C and 30–40%. The polymer solution was completely volatilized during electrospinning. The resulting nanofiber mats were collected from the aluminum foil plates and stored in a dry environment for further use.

2.3. Characterization of polymer solutions

The pH was measured using a PHS-3C pH meter (Leici, Shanghai, China). Conductivity levels were assessed using a Delta 326 digital conductivity meter (Mettler-Toledo, Zurich, Switzerland). The viscosities of the polymer solutions were measured using an NDJ-8S viscometer (PingXuan, Shanghai, China). All polymer solutions were measured at room temperature (25 °C) in triplicate over a measuring time of 2 min at a speed of 60 rpm.(Alehosseini, Sarabi-Jamab, Ghorani, & Kadkhodaee, 2019).

2.4. Scanning electronic microscopy

The electrospun nanofibers were observed using SEM (SN-3400, Hitachi, Tokyo, Japan) using a previously describe previous method (Librán et al., 2017). The prepared nanofiber samples were coated after bonding them to the substrate using gold spraying and then observed using SEM. Using ImageJ, the diameters of 100 randomly selected nanofibers, and SEM images were obtained at a magnification of 5000×. The fiber diameter distribution map was plotted using the Origin software (version 9.0; Origin Lab, USA).

2.5. Attenuated total reflection-flourier transform infrared spectroscopy (ATR-FTIR)

The infrared spectra of the MFGM, WPI, and PUL powders, as well as various ratios of MFGM/PUL and WPI/PUL nanofibers, were obtained using Fourier transform infrared spectrometer (FTIR, iS50, Thermo

Science, Waltham, MA, USA). The resolution was set to 4 cm^{-1}, and the spectral acquisition ranged from 4000 cm^{-1} to 500 cm^{-1}. Spectral acquisition was repeated 32 times.

2.6. X-ray diffraction (XRD)

The XRD patterns of the MFGM, WPI, and PUL powders, as well as different ratios of MFGM/PUL and WPI/PUL nanofibers, were obtained using an X-ray diffractometer (PANalytical, X'pert PRO Multi-purpose X-ray diffractometer, Almelo, The Netherlands). The XRD instrument was calibrated using Cu-Kα radiation, with a voltage setting of 40 kV and a current of 30 mA. The scan angle ranged from 5° to 85° (2θ) with a scan rate of 2°/min (Xu, Ban, et al., 2022). The obtained data were analyzed using JADE software (Redwood Shores, CA, United States).

2.7. Thermogravimetric analysis

Changes in the weight loss of the MFGM, WPI, PUL powder, and nanofibers were determined by TGA (SDT-650, TA Instruments Co., Ltd., New Castle, DE, USA) according to a previously described method (Ma et al., 2021). The powders of MFGM, WPI, PUL, and nanofibers of MFGM/PUL and WPI/PUL (10 mg) were subjected to controlled heating by increasing the temperature from 25 to 700 °C in a nitrogen-rich environment. The heating was changed at a rate of 10 °C/min.

2.8. Mechanical properties

Tensile strength (TS) and elongation at break (EAB) are two important indices that reflect the tensile properties of a material. A slight modification of this method was made with reference to Li et al. (2024). The nanocomposite fiber membranes were cut into 50 mm × 20 mm pieces and fixed with an A/MTG fixture using a TA.XT-Plus type mass tester (Stable Micro Systems, UK). The initial distance of the fixture was set to 40 mm, and the ultimate stretching distance was 100 mm at a stretching speed of 0.5 mm/s-1. Three mechanical measurements were performed on each membrane sample. The TS and EAB values of the nanofiber films were calculated using to Eqs. (1) and (2) (Chen, Liu, Deng, Zhou, & Hong, 2022).

$$TS(\mathrm{MPa}) = \frac{F_{max}}{s} \tag{1}$$

$$EAB(\%) = \frac{L_f - L_0}{L_0} \times 100\% \tag{2}$$

2.9. Preparation of nanofiber-encapsulated LGG

LGG was inoculated into MRS broth and followed by a 24-h incubation at 37 °C. After incubation, cells were centrifuged, washed with sterile water and collected. The collected sample were added to the polymer solution to obtain a final concentration of 8 log CFU/g. The polymer solution containing with LGG was electrospun as described above.

2.10. Distribution observations of nanofiber-encapsulated LGG by fluorescence microscopy

For fluorescence microscopy, the samples were prepared according to a previously described method (Xu et al., 2022). Nanofiber encapsulated LGG was stained with rhodamine 123 (Solarbio Technology Co., Ltd., Beijing, China) staining solution (5 μg /mL) in the dark at 37 °C for 1 h. After this incubation, the cells were centrifuged at 4000 ×*g* for 5 min at 4 °C, and rinsed thrice times with sterile water to remove residual rhodamine 123 dye. All steps were performed under light-protected conditions to avoid dye quenching. The distribution of LGG within the nanofiber membrane was observed using fluorescence microscopy (DMi8, Leica, Germany) and SEM.

2.11. Survivability and storage stability of nanofiber-encapsulated LGG

Nanofiber-encapsulated LGG was diluted ten times with PBS (*w/v*). The survival of nanofiber-encapsulated LGG in simulated gastric juice (pH = 3.0) and simulated intestinal juice (pH = 6.8) was determined as described previously (Minekus et al., 2014). Pepsin (1% w/v) and trypsin (1% w/v) solutions were prepared. The tolerance of nanofiber-encapsulated LGG to bile salts was determined in accordance with an established protocol; 0.3% (w/v) bile salt solution was used (Adesulu-Dahunsi, Jeyaram, & Sanni, 2018). The storage stability of nanofiber-encapsulated LGG was determined in a cold room (4 °C) and at room temperature (25 °C). The number of live bacteria was determined at 0, 7, 14, 21, and 28 d of storage.

2.12. Statistical analysis

Each experimental sample was independently replicated three times. All data were expressed as mean ± standard deviation. Data analysis was performed using SPSS Statistics software (version 19.0), and a one-way analysis of variance was performed using Tukey's method ($P < 0.05$). Student's *t*-test at 95% confidence level was used for data analysis and Origin 2019 was used to generate graphs.

3. Results and discussion

3.1. Physicochemical properties of polymer solutions

pH adjustment is important for the electrospun encapsulation of lactobacilli. The pH of the solution has two effects: first, it affects the solubility of the polymer, and second, it prevents a decrease in lactobacillus activity, which tends to occur at excessively low pH levels (Ebadi Nezhad, Edalatian Dovom, Habibi Najafi, Yavarmanesh, & Mayo, 2020). Therefore, we investigated pH changes in the polymer solution. As shown in Table 1, the pH of the pure PUL solution was 4.74 ± 0.03. By modulating the ratio of MFGM and WPI in the blended polymer ($P < 0.05$), it was possible to significantly elevate the pH of the polymer solution to the range of 5.5 to 6.0. Researchers have demonstrated that varying polymer ratio from 9:1 to 6:4 result in a decrease in encapsulated *Lacticaseibacillus* survival from 89.26% to 76.58%. When the pH of the solution exceeded 4.0, nearly all *Lacticaseibacillus* strains could tolerate the encapsulation process (Ebadi Nezhad et al., 2020). The pH of the polymer solutions used in this study was >4.0, indicating that the pH of both MFGM/PUL and WPI/PUL polymer solutions had minimal adverse effects on the viability of the *Lacticaseibacillus*.

The viscosity and conductivity of the polymer solution affect the electrospinning process. The appearance and spinnability of the fiber and the viscosity of the solution are directly affected by the conductivity and composition of the polymer solution (Tiwari & Venkatraman, 2012). The viscosity of a solution is a clear indicator of the degree of entanglement between the polymer molecules within the chain. The results in Table 1 show that the MFGM solution (MFGM: PUL = 100:0) had a viscosity of 282.34 ± 4.28 mPa.s, whereas the viscosity of the WPI solution (WPI: PUL = 100:0) remained undetectable. It was also shown that the MFGM solution existed in an emulsion state. However, increasing the PUL content significantly increased the viscosity of both MFGM/PUL and WPI/PUL polymer solutions ($P < 0.05$). This unequivocally indicated increased interactions between MFGM, WPI, and PUL. MFGM and WPI are byproducts of whey produced during the processing of butter and cheese. The high viscosity of MFGM compared with that of WPI is ascribable to its high content of polar phospholipids, which form a highly viscous paste when dissolved.

Furthermore, the data indicated that the conductivity of pure PUL solution was 0.33 ± 0.02 mS/cm and that increasing the content of MFGM and WPI led to a significant increase in the conductivity of the

Table 1
pH, Viscosity, and conductivity of different ratio milk fat globule membrane (MFGM)/pullulan (PUL) and whey protein isolates (WPI)/ pullulan (PUL) blended solutions.

MFGM/PUL (*w*/w)	pH	Conductivity (mS/cm)	Viscosity (mPa·s)	WPI/PUL (w/w)	pH	Conductivity (mS/cm)	Viscosity (mPa·s)
0:100	4.74 ± 0.03^{a}	0.33 ± 0.02^{a}	1465.33 ± 9.02^{a}	0:100	4.74 ± 0.03^{a}	0.33 ± 0.02^{a}	1465.33 ± 9.02^{a}
20:80	5.49 ± 0.01^{b}	0.41 ± 0.03^{b}	1242.67 ± 7.57^{b}	20:80	5.60 ± 0.02^{b}	0.42 ± 0.02^{b}	876.00 ± 4.00^{b}
30:70	5.65 ± 0.02^{c}	0.52 ± 0.03^{c}	991.33 ± 4.16^{c}	30:70	5.63 ± 0.01^{b}	0.56 ± 0.02^{c}	564.67 ± 6.43^{c}
40:60	5.67 ± 0.01^{c}	0.59 ± 0.01^{d}	970.33 ± 4.73^{d}	40:60	5.68 ± 0.02^{c}	0.72 ± 0.01^{d}	404.67 ± 8.08^{d}
50:50	5.69 ± 0.01^{cd}	0.66 ± 0.02^{e}	924.67 ± 7.57^{e}	50:50	5.71 ± 0.02^{cd}	0.87 ± 0.02^{e}	233.33 ± 6.11^{e}
60:40	5.73 ± 0.02^{de}	0.73 ± 0.01^{f}	736.67 ± 9.87^{f}	60:40	5.75 ± 0.01^{d}	1.08 ± 0.03^{f}	126.67 ± 6.43^{f}
70:30	5.77 ± 0.02^{e}	0.87 ± 0.02^{g}	636.67 ± 7.02^{g}	70:30	5.85 ± 0.02^{e}	1.23 ± 0.02^{g}	86.67 ± 3.06^{g}
80:20	5.82 ± 0.02^{f}	1.09 ± 0.01^{h}	411.00 ± 7.00^{h}	80:20	5.96 ± 0.02^{f}	1.41 ± 0.02^{h}	46.00 ± 2.00^{h}
100:0	5.94 ± 0.01^{g}	1.20 ± 0.03^{i}	282.34 ± 4.28^{i}	100:0	6.08 ± 0.02^{g}	1.59 ± 0.01^{i}	–

Values with a different superscript letter in the same column indicate significantly different ($P < 0.05$).

polymer solution, which is attributed to the interaction between MFGM/WPI and PUL ($P < 0.05$). Studies have shown that as the PUL content increases, hydrogen bonding between proteins and polysaccharide molecules increases, which in turn increases viscosity (Kriegel, Arrechi, Kit, McClements, & Weiss, 2008). Conversely, a decrease in the relative amount of PUL leads to an increase in the polyelectrolyte nature of the protein and consequently a decrease in conductivity (Jia et al., 2020).

Therefore, the morphology of electrospun nanofibers depends on several factors. It has been shown that the higher the solution viscosity, the larger the fiber diameter. As the conductivity of the solution increases, the diameter of the electrospun nanofibers decreases significantly, which is consistent with our experimental results (Haghi & Akbari, 2007). This suggests that as the PUL content increased, the comingled solution formed with MFGM/WPI formed electrospun fibers with larger diameters under electrostatic action, which we needed to further confirm by electron microscopy.

3.2. Morphological characterization of nanofibers

SEM was used to observe and analyze the morphology and diameter distribution of the nanofiber membranes generated by electrostatic forces from the polymer solutions of MFGM/PUL and WPI/PUL at different weight ratios. As shown in Fig. 1a, the diameter of the pure PUL nanofiber membrane was uniformly distributed at 281.01 ± 57.95 nm. The fiber diameters decreased to 167.03 ± 84.39 nm (Fig. 1h) and 140.26 ± 53.12 nm (Fig. 1o) for MFGM/PUL (80:20) and WPI/PUL (80:20) blends, respectively. It is worth noting that with a weight ratio of MFGM/PUL and WPI/PUL of 20:80, a uniform diameter distribution is achieved in the nanofiber membranes, with nanofiber diameters of 270.02 ± 56.42 nm (Fig. 1b) and 263.21 ± 55.12 nm (Fig. 1i), respectively. It can be seen by SEM micromorphology that with the proportion of MFGM and WPI in the blend system increasing from 20% to 80%, the incidence of nanofiber "beads" increases, and the fiber thickness is not uniform. However, as the content of MFGM increased and the content of PUL decreased, the fiber diameter showed a downward trend, suggesting that reducing the ratio of PUL affected the interaction between the two biopolymers, indicating that the protein molecules were not sufficiently involved in entanglement or interchain binding (Colín-Orozco, Zapata-Torres, Rodríguez-Gattorno, & Pedroza-Islas, 2015).

In particular, when pure solutions of MFGM and WPI were used, the electrospinning process resulted in droplet formation, suggesting that they were unsuitable as electrospinning materials. This result, together with the findings of previous researchers who consistently observed that whey protein alone produced droplets and failed to form fibrous structures, led to interesting discoveries during the production of pea protein isolate-pullulan blend electrospun nanofiber films. Pea protein isolates alone lacked the ability to form a fibrous film (Jia et al., 2020). The formation of nanofibers was successfully facilitated by the introduction of PULs. This phenomenon can be attributed to the inherent limitations of aqueous protein solutions, especially those with globular protein molecules, which lack the entanglements or interchain associations necessary for fibrous structure formation during electrospinning. The incorporation of a spinnable polymer, such as PUL, effectively addresses this challenge, and facilitates the formation of composite fibers (López-Rubio, Sanchez, Sanz, & Lagaron, 2009).

3.3. Attenuated total reflection-Fourier transform infrared analysis of nanofiber

The infrared spectra of MFGM, WPI, and PUL powders and different weight ratios of MFGM/PUL and WPI/PUL nanofibers are shown in Fig. 2. Both the MFGM and WPI powders exhibited a distinct absorption peak at 3278 cm^{-1}, that is characteristic of the stretching vibration of the O—H stretching spectral band. In addition, the intensity of the absorption peak at 3278 cm^{-1} was higher for MFGM than for WPI, indicating the deepening of hydrogen bonds in MFGM (Qin, Jia, Liu, Kong, & Wang, 2020). Upon the addition of PUL, the peak shifted, indicating that the absorption band was affected by intermolecular or intramolecular hydrogen bonding, suggesting that PUL formed hydrogen bonds with MFGM and WPI (Jia et al., 2020). In addition, the characteristic absorptions of MFGM and WPI at 1631 and 1528 cm^{-1} corresponded to the C═O stretching vibration of amide I and the N—H bending and C—N stretching vibrations of amide II respectively (Drosou et al., 2018). When PUL was added, the spectral bands of amides I and II displayed a blue shift, suggesting electrostatic interactions between the hydroxyl groups of PUL and the amino groups of MFGM and WPI (Jia et al., 2007). Meanwhile, MFGM powder showed a robust absorption band corresponding to P═O stretching vibration at 1300–1140 cm^{-1} and a distinct C═O stretching vibration at 1742 cm^{-1}, indicating that MFGM has a higher content of phospholipids compared to WPI (Drosou et al., 2018). The result showed that when the proportion of PUL in blended fibers increased from 50% to 80%, PUL provided more hydroxyl groups to strongly interact with the amino groups of MFGM and WPI, and the amide I and II bands moved towards higher wave numbers (Fig. 2), which was conducive to fiber formation.

3.4. X-ray diffraction patterns analysis of nanofibers

To optimize polymer crystallinity, destructive and constructive interferences within the diffraction pattern were analyzed using through X-ray diffraction (Joye & McClements, 2014). The XRD patterns of the MFGM, WPI, PUL powders, MFGM/PUL, and WPI/PUL nanofibers compositions, each with varying weight ratios were studied (Fig. 3). Upon further examination, the distinctive reflections at 19.03°, 19.43°, and 18.57°, attributed to the MFGM, WPI, and PUL powders, respectively, appeared as distinct diffraction peaks indicative of amorphous structures (Luo et al., 2022). In addition, the introduction of MFGM/PUL and WPI/PUL resulted in distinct attributes within the XRD patterns of the nanofibers compared with the powder forms. These attributes manifested as broadened and diminished diffraction peaks,

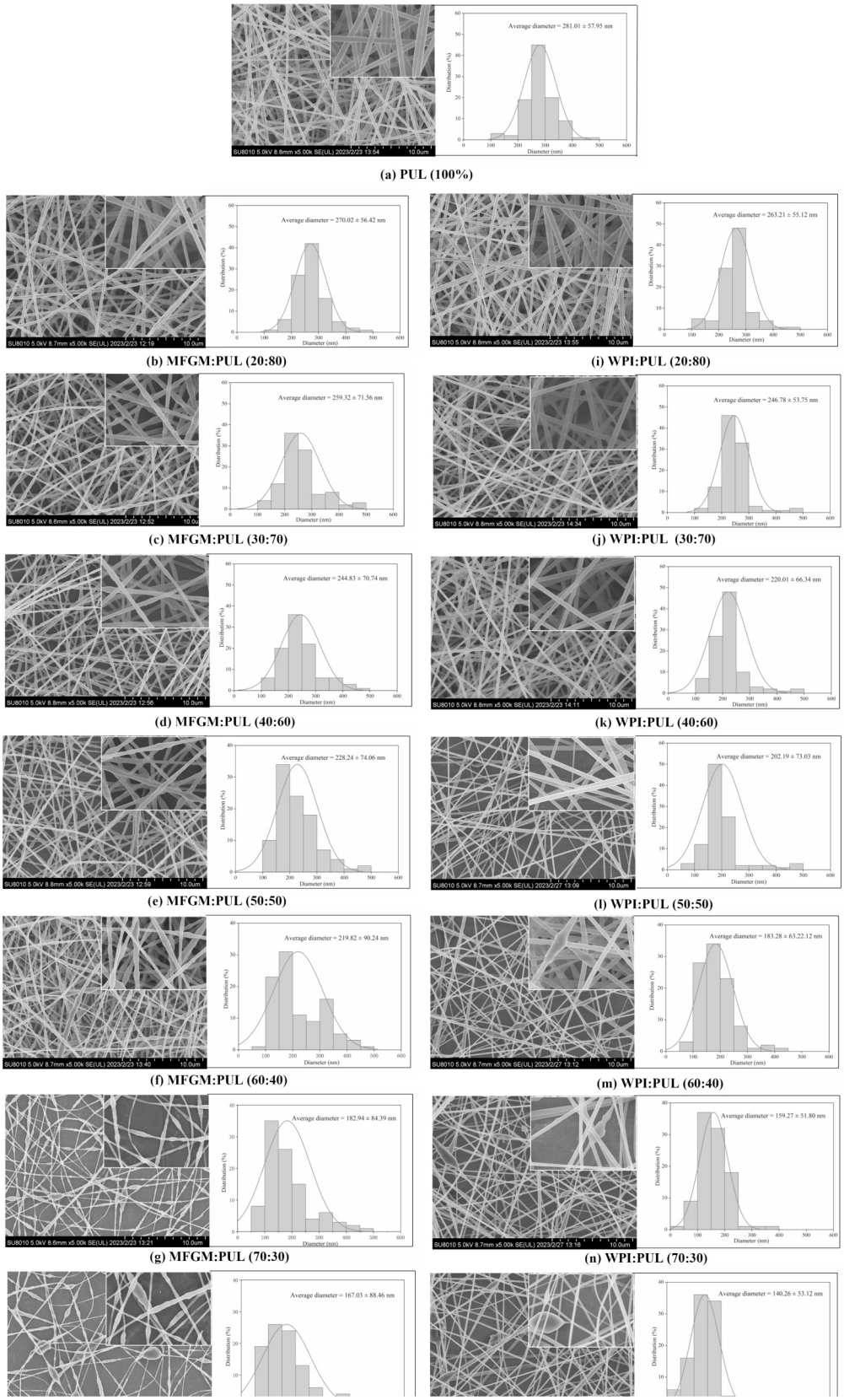

Fig. 1. Scanning Electron Microscope (SEM) micrographs and fiber diameters of electrespun nanofibers. (a) PUL (100%), (b) MFGM/PUL(20:80), (c) MFGM/PUL (30:70), (d) MFGM/PUL(40:60), (e) MFGM/PUL(50:50), (f) MFGM/PUL(60:40), (g) MFGM/PUL(70:30), (h) MFGM/PUL(80:20) and (i) WPI/PUL(20:80), (j) WPI/PUL(30:70), (k) WPI/PUL(40:60), (l) WPI/PUL(50:50), (m) WPI/PUL(60:40), (n) WPI/PUL(70:30), (o) WPI/PUL(80:20). Fiber diameters of the electrospun fibers were measured by ImageJ software from the SEM images obtained at a magnification of 5000 × .

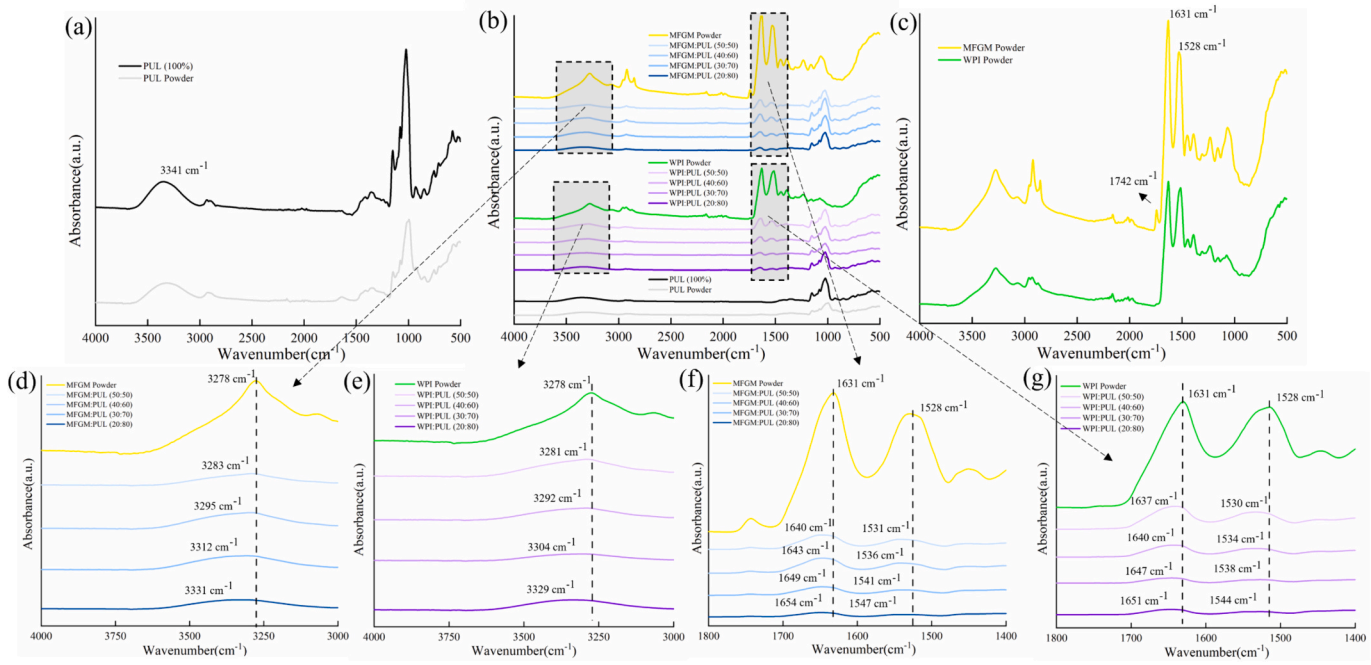

Fig. 2. Attenuated total reflection-Fourier transform infrared (ATR-FTIR) of pullulan (PUL) powder, milk fat globule membrane (MFGM) powder, whey protein isolates (WPI) powder and different weight ratios of MFGM/PUL and WPI/PUL nanofibers.

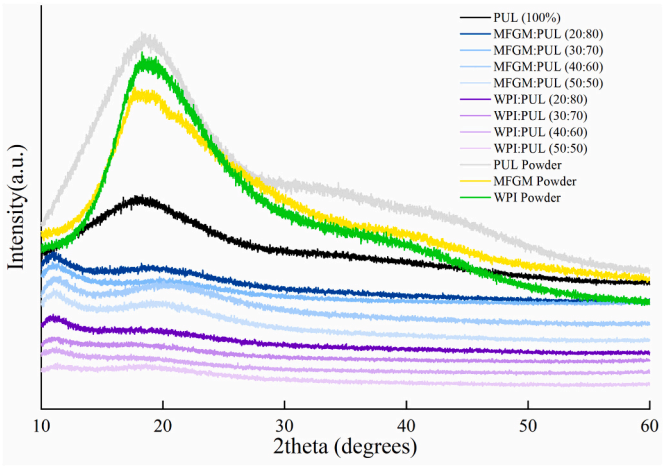

Fig. 3. X-ray diffraction (XRD) patterns of pullulan (PUL) powder, milk fat globule membrane (MFGM) powder, whey protein isolates (WPI) powder and different weight ratios of MFGM/PUL and WPI/PUL nanofibers.

accompanied by a small angular shift. These phenomena are ascribable to the interaction between MFGM/WPI and PUL molecules (Jia et al., 2007; Qin, Jia, Liu, Kong, & Wang, 2019). Consistent with prior research findings, the XRD analysis demonstrated that electrospinning retards crystallization while concurrently facilitating the development of an amorphous polymer structure. The resulting MFGM/PUL and WPI/PUL composites exhibited distinct amorphous characteristics, confirming this finding. The experimental results combined with ATR-FTIR confirmed that MFGM/WPI had electrostatic interaction and hydrogen bond interaction with PUL molecules to form nanofibers.

3.5. Thermal stability analysis of nanofibers

TGA is the process of changing a residual substance with temperature or time. Fig. 4a, depicts the TGA profiles of various samples, including the MFGM, WPI, PUL powders, and MFGM/PUL and WPI/PUL nanofibers. The results showed two distinct stages of weight loss. The initial weight loss of around 100 °C was attributed to water evaporation, while the subsequent weight reduction between 200 °C and 450 °C was mainly due to the thermal degradation of polysaccharides and proteins in the samples (Xiao & Lim, 2018).

The derivative thermogravimetric analysis (DTG) curve shows the relationship between weight loss rate and temperature (or time). The DTG data in Fig. 4b highlight that the temperature corresponding to the maximum weight loss rate for PUL fiber (293.14 °C) was higher than that of PUL powder (290.42 °C). Similar observations have been reported in other studies, such as for pea protein isolates/PUL blended fibers (Jia et al., 2020). This phenomenon illustrates the electrospinning process enhancement the intermolecular interactions by electrospinning, which leads to increased thermal stability within the resulting fibers (Aceituno-Medina, Lopez-Rubio, Mendoza, & Lagaron, 2013). The thermal stabilities of MFGM/PUL and WPI/PUL nanofibers were related to the composition of the mixed solution. When the ratio of MFGM to WPI in the mixed solution decreased from 50% to 20%, the temperature corresponding to the maximum weight loss of the nanofibers increased gradually, and the corresponding stability decreases gradually. When the mass ratio of MFGM/PUL and WPI/PUL was adjusted to 20:80, the peak weight loss temperatures of the nanofibers were 302.12 and 300.54 °C, respectively, which were the most stable and not easily degraded among all polymer concentrations. Therefore, the experimental results confirm that the interaction of the MFGM/PUL and WPI/PUL composite fiber nanomembranes changes the degradation characteristics of the membranes, and the composite nanofibers can be processed at high temperatures and are practicability.

3.6. Mechanical properties analysis of nanofibers

The mechanical property parameters of the nanofiber membranes with different ratios are shown in Table 2, which indicates that different ratios of polymer solutions of MFGM/PUL and WPI/PUL have a significant effect on the mechanical properties of the composite nanofibers ($P < 0.05$). The tensile strength of pure PUL nanofibers was about 11.49 ± 1.13 MPa and the elongation at break was 16.03% ± 1.52%. Therefore, the SEM and static tensile test results showed that the electrospun film

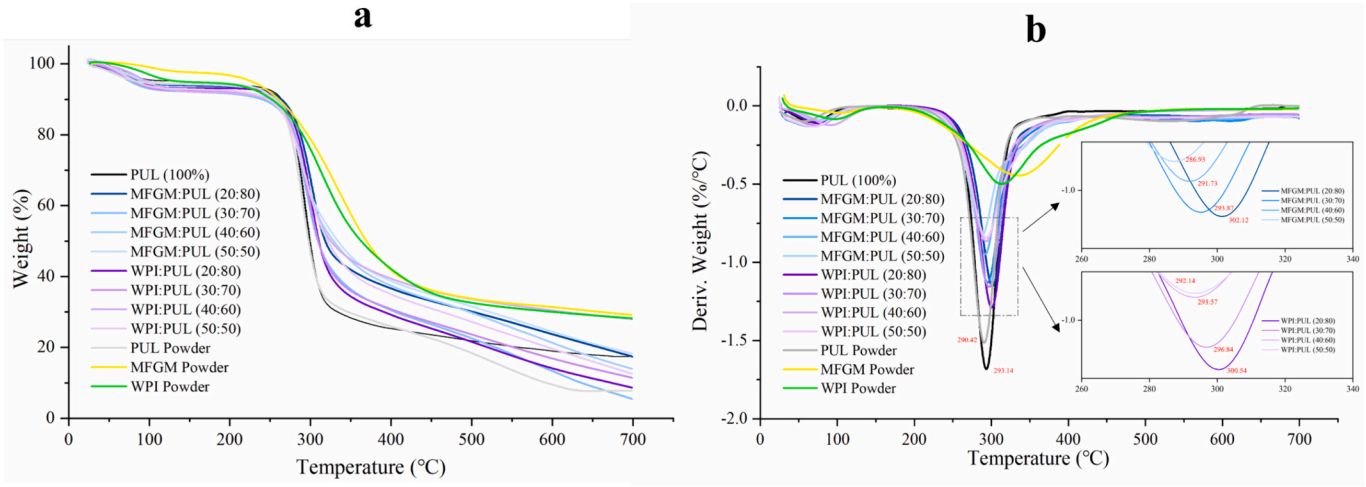

Fig. 4. Properties of pullulan (PUL) powder, milk fat globule membrane (MFGM) powder, whey protein isolates (WPI) powder and different weight ratios of MFGM/PUL and WPI/PUL nanofibers (a) Thermogravimetric analysis (TGA) curves; (b) Derivative Thermogravimetry (DTG) curves.

Table 2
The mechanical properties of the milk fat globule membrane (MFGM)/pullulan (PUL) and whey protein isolates (WPI)/ pullulan (PUL) nanofiber.

MFGM/ PUL (w/w)	Tensile strength (Mpa)	Elongation at break (%)	WPI/ PUL (w/w)	Tensile strength (Mpa)	Elongation at break (%)
0:100	11.49 ± 1.13^{Aa}	16.03 ± 1.52^{Aa}	0:100	11.49 ± 1.13^{Aa}	16.03 ± 1.52^{Aa}
20:80	10.92 ± 0.91^{Aa}	13.67 ± 1.21^{Ab}	20:80	10.69 ± 0.92^{Aa}	11.09 ± 1.06^{Bb}
30:70	9.10 ± 0.47^{Ab}	8.32 ± 0.42^{Ac}	30:70	7.86 ± 0.56^{Bb}	7.19 ± 0.63^{Bc}
40:60	6.26 ± 0.30^{Ac}	5.34 ± 0.28^{Ad}	40:60	4.57 ± 0.41^{Bc}	3.88 ± 0.39^{Bd}
50:50	2.51 ± 0.28^{Ad}	2.85 ± 0.33^{Ae}	50:50	1.57 ± 0.20^{Bd}	2.04 ± 0.22^{Be}

Capital letters (A-B) indicate statistically significant differences in mechanical properties between MFGM/PUL and WPI/PUL at the same ratio ($P < 0.05$). Lowercase letters (a-d) indicate statistically significant differences in mechanical properties of MFGM/PUL and WPI/PUL at different ratios ($P < 0.05$).

had a good microstructure and macroscopic mechanical strength in the polymer solution with MFGM/PUL and WPI/PUL ratio of 20:80. PUL is a natural crosslinking agent, that can bind to proteins through hydrogen bonding. The addition of PUL reduces the fluidity of proteins, increases the interaction between molecules, leads to a decrease in elongation at break and an increase in tensile strength (Karim et al., 2009). However, high levels of MFGM and WPI can electrospinning, which leads to increased, and aggregation occurs in the film, resulting in a decrease in tensile strength; similar results have been reported by Wang et al. (2019). These results also indicate the formation of hydrogen bonds between MFGM, WPI, and PUL, which was confirmed by FTIR and XRD analysis.

3.7. Distribution of nanofiber-coated LGG observed via SEM and fluorescence microscopy

Based on the above experimental results, the optimum MFGM/PUL and WPI/PUL ratios were determined to be 20:80. SEM and fluorescence microscopy were used to observe the distribution of LGG within the polymer nanofibers. As shown in Fig. 5 **c** and **f**, the successful

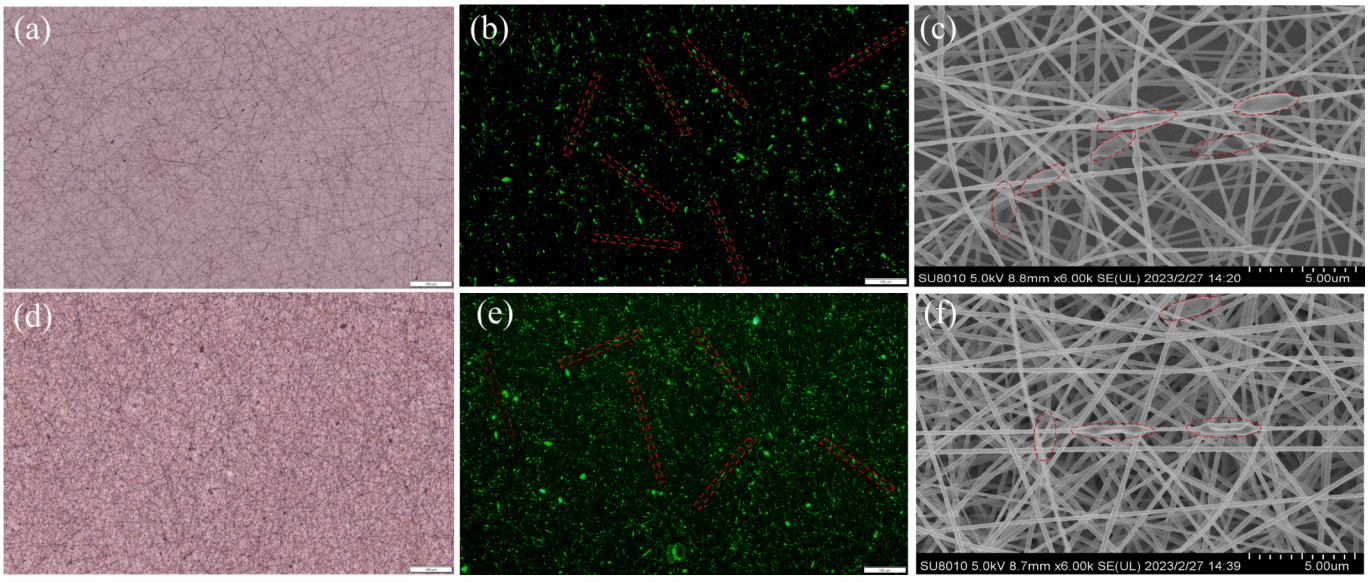

Fig. 5. Micrographs of *Lacticaseibacillus rhamnosus* GG staining encapsulated in milk fat globule membrane (MFGM)/pullulan (PUL) nanofibers and whey protein isolates (WPI)/pullulan (PUL) at the ratio of 20:80, respectively. (a&d) Optical micrographs, (b&e) Fluorescence micrographs, (c&f) SEM images.

encapsulation of LGG within the nanofibers is evident. These results were consistent with the findings of a similar study (Yilmaz, Taylan, Karakas, & Dertli, 2020). Consistent with these findings, the presence of LGG was associated with localized fiber thickening in an elliptical pattern, noticeable diameter enlargement, darker pigmentation, random dispersion across multiple fibers and longitudinal alignment within individual fibers. This stems from the behavior of the LGG-infused mixture, which forms a Taylor cone under the influence of a high-voltage electric field. This process led to directional LGG flow, subsequent encapsulation within the fiber matrix, and rapid solvent evaporation (Fung, Yuen, & Liong, 2011). In addition to SEM imaging, the distribution of LGG was observed using fluorescence microscopy, as shown in Fig. 5a, b, d, and e. The presence of green fluorescence, resulting from the aggregation of rhodamine 123 dye within the LGG mitochondrial matrix, became apparent when viewed under a fluorescence microscope. A substantial portion of LGG was successfully encapsulated within both MFGM/PUL and WPI/PUL fibers (Fig. 5 **b, and e red dotted line**). However, a small amount of LGG was observed outside the blended fiber structure. In previous studies, PVC/PEC fibers were able to encapsulate L. *rhamnosus*, but were not fully encapsulated by the fibers, which is consistent with our experimental results (Xu, Ma, et al., 2022).

3.8. Survivability and storage stability of nanofiber-encapsulated LGG

Changes in the viability of the MFGM/PUL nanofibers before and after LGG encapsulation were further investigated. As shown in Table 3, the viability of the encapsulated LGG by fibrous membranes formed by all polymer solutions after the addition of electrostatics was significantly reduced ($P < 0.05$), suggesting that the electrostatic spinning process had a significant influence on cell viability. However, no significant difference was noted in the activity of the LGG-blended materials after electrospinning-based encapsulation ($P > 0.05$). This decrease in activity can be attributed to the combined influence of increased voltage and osmotic stress caused by rapid water evaporation during electrospinning (Mojaveri, Hosseini, & Gharsallaoui, 2020). This observation suggests that the three polymer solutions had an insignificant effect on the amount of *Lacticaseibacillus* (Ma et al., 2021). The described method has been employed by various researchers to embed diverse *Lacticaseibacillus* and among them, the survival rates of *L. acidophilus* and *L. plantarum* were significantly higher after electrospinning-based embedding than those of the other strains. This difference in survival rates may be attributed to differences in the structural characteristics of bacteria such as S-layer protein, teichoic acid, capsular polysaccharide, and peptidoglycan composition among the different strains (Zaeim, Sarabi-Jamab, Ghorani, Kadkhodaee, & Tromp, 2018).

To further confirm the protective effect of the MFGM/PUL nanofibers on LGG, LGG tolerance was assessed under three treatment conditions: gastric juice, intestinal juice, and bile salt. Table 4 shows the quantified viable bacterial counts when LGG was exposed to MFGM/PUL, WPI/PUL, and PUL nanofibers for different time intervals. Compared with the viable LGG count within pure PUL nanofibers, MFGM/PUL and WPI/PUL nanofibers showed significant improvements in the tolerance of LGG to gastric juice, intestinal juice, and bile salts. Interestingly, after 3 h of treatment, the number of viable LGG encapsulated within the MFGM/PUL nanofibers was significantly higher than that within the WPI/PUL nanofibers ($P < 0.05$). This demonstrates the improvement attributed to the presence of MFGM in improving the tolerance of LGG against the challenges caused by gastric and intestinal juices, as well as bile salts. The consistency of our results with those of previous studies further substantiated our findings (Zhang et al., 2020). The presence of MFGM increased the thickness of LGG biofilms under stress conditions and played a protective role.

Table 5 shows the variations in LGG viable population during the storage period of LGG samples made of MFGM/PUL nanofibers at temperatures of 4 and 25 °C for 28 days. Overall, the viable LGG counts demonstrated a decreasing trend with increasing storage time, and the LGG survival during storage at 4 °C was better than that at 25 °C. After 28 days of storage at 4 and 25 °C, the viable LGG counts in MFGM/PUL nanofiber were significantly higher than those in WPI/PUL and PUL fibers ($P < 0.05$), indicating that MFGM was superior to WPI as a spinning aid. This observation also indicate that different packaging materials have different effects on the survival count of *Lacticaseibacillus* during

Table 3
Vitality changes of*Lacticaseibacillus rhamnosus* GG in different blended materials before and after electrostatic spinning process.

	Viability (log CFU/g)	
	Control	Electrospinning
MFGM/PUL (20:80)	8.36 ± 0.09^{Aa}	7.22 ± 0.13^{Ab}
WPI/PUL (20:80)	8.29 ± 0.21^{Aa}	7.28 ± 0.10^{Ab}
PUL (100%)	8.31 ± 0.18^{Aa}	7.24 ± 0.15^{Ab}

Capital letters (A) indicate statistically significant ($P < 0.05$) differences in viability between the different co-mingled materials. Lowercase letters (a-b) indicate statistically significant ($P < 0.05$) differences in LGG survival between before and after encapsulation.

Table 4
Gastric, intestinal fluid and bile salt tolerance of*Lacticaseibacillus rhamnosus* GG encapsulated by different co-mingled fibers.

Treatment	Time	Viability (log CFU/g)		
		MFGM/PUL (20:80)	WPI/PUL (20:80)	PUL (100%)
Non treatment	–	7.22 ± 0.13^{Aa}	7.28 ± 0.10^{Aa}	7.24 ± 0.15^{Aa}
gastric juice	30 min	6.59 ± 0.18^{Ba}	6.55 ± 0.15^{Ca}	6.48 ± 0.07^{Ba}
	3 h	6.39 ± 0.12^{Ca}	5.52 ± 0.18^{Db}	5.45 ± 0.12^{Cb}
Intestinal juice	30 min	6.64 ± 0.11^{Bab}	6.77 ± 0.10^{Ba}	6.57 ± 0.21^{Bb}
	3 h	6.53 ± 0.14^{BCa}	5.37 ± 0.12^{Db}	5.21 ± 0.18^{Dc}
Bile salt	30 min	5.74 ± 0.13^{Da}	5.43 ± 0.10^{Db}	5.23 ± 0.19^{CDc}
	3 h	5.38 ± 0.14^{Ea}	5.15 ± 0.16^{Eb}	4.52 ± 0.11^{Ec}

Capital letters (A-E) indicate statistically significant differences ($P < 0.05$) in the viability of LGG encapsulated in the same material under different treatment conditions. Lowercase letters (a-c) indicate statistically significant differences ($P < 0.05$) in the viability of LGG encapsulated in different encapsulated materials under the same treatment conditions.

Table 5
Viability of*Lacticaseibacillus rhamnosus* GG in different nanofibers stored for 28 days at 4 °C and 25 °C.

	Viability (log CFU/g)					
	4 °C			25 °C		
	MFGM/PUL (20:80)	WPI/PUL (20:80)	PUL (100%)	MFGM/PUL (20:80)	WPI/PUL (20:80)	PUL (100%)
0 d	7.22 ± 0.13^{Aa}	7.28 ± 0.10^{Aa}	7.24 ± 0.15^{Aa}	7.22 ± 0.13^{Aa}	7.28 ± 0.10^{Aa}	7.24 ± 0.15^{Aa}
7 d	7.06 ± 0.12^{Aa}	6.96 ± 0.10^{Bab}	6.77 ± 0.13^{Bcd}	6.87 ± 0.13^{Bbc}	6.65 ± 0.17^{Bd}	6.36 ± 0.14^{Be}
14 d	6.80 ± 0.09^{Ba}	6.52 ± 0.08^{Cb}	6.24 ± 0.07^{Cc}	6.45 ± 0.11^{Cb}	6.15 ± 0.08^{Cc}	5.72 ± 0.14^{Cd}
21 d	6.43 ± 0.14^{Ca}	6.04 ± 0.11^{Db}	5.52 ± 0.19^{Dc}	6.02 ± 0.15^{Db}	5.54 ± 0.19^{Dc}	5.09 ± 0.21^{Dd}
28 d	6.06 ± 0.15^{Da}	5.47 ± 0.14^{Eb}	4.71 ± 0.13^{Ec}	5.47 ± 0.12^{Eb}	4.64 ± 0.18^{Ec}	4.28 ± 0.14^{Ed}

Capital letters (A-E) indicate statistically significant difference ($P < 0.05$) in storage viability of LGG encapsulated with the same material at different times at the same temperature. Lowercase letters (a-d) indicate statistically significant difference ($P < 0.05$) in storage viability of LGG encapsulated at different temperatures on the same days.

storage (Ashwar, Gani, Gani, Shah, & Masoodi, 2018). Notably, the survival rates of LGG measured at the different temperatures for 28 days were 83.9% and 75.8%, respectively, indicating that some of the substances in the MFGM/PUL nanofibers play a protective role against LGG, and we speculate that it may be the phospholipids in MFGM that play a role, which needs to be further investigated in the future.

MFGM is a complex three-layer lipoprotein membrane composed of polar lipids, cholesterol, and proteins. It has been the subject of considerable interest due to its emulsifying properties and potential as a bioactive ingredient (Lopez, 2011). In particular, the phospholipids in MFGM are capable of interacting with proteins, and over time bacterial cells can become embedded in MFGM and become part of the phospholipid bilayer, making it potentially useful for encapsulating probiotics (Wu et al., 2022). The results of FTIR experiments demonstrated that MFGM contains phospholipids compared to WPI. Thus, the formation of the liposome structure exhibits higher thermal stability, which serves to protect and deliver sensitive bioactivities, improve the stability of the nanofibrous membrane and thus potentially reduce gastric lipolysis (Yao, Ranadheera, Shen, Wei, & Cheong, n.d.). The formation of nanofibrous films is facilitated by strong molecular interactions between PUL and MFGM in the presence of electrostatic forces, a process that does not destroy the protein structure and that allows PUL to participate in the attachment not only as a reactant but also as a protective layer for whey proteins with the functional properties of the glycoproteins produced (Ali et al., 2023). In addition, our previous studies have demonstrated that MFGM increased glucose and sucrose transport through multiple metabolic pathways, ameliorated bifidobacterial shrinkage, fragmentation and irregular morphology under bile salt stress, maintained cellular integrity and promoted probiotic mobility, and the synergistic and complementary effects of MFGM and probiotics have a synergistic effect on mucosal immunity (Cherbut et al., 2004; Li et al., 2019; Zhang et al., 2024). In conclusion, the encapsulation of LGG by MFGM/PUL nanofibrous membranes is feasible and can improve LGG survival in the gut and reduce damage from environmental stressors. These results provide a new approach for the preparation of MFGM/PUL as a food-grade material for encapsulation of probiotics in nanofibrous membranes, which is expected to be applied in the food industry.

4. Conclusion

In this study, food-grade nanofibers derived from an aqueous solution of MFGM/PUL were developed using electrospinning for the first time. The MFGM/PUL ratio significantly affected on the pH, conductivity and viscosity of the mixed solution ($P < 0.05$). SEM analysis confirmed that increased PUL content contributed to the formation of nanofibers with uniform diameter. Fourier transform infrared spectroscopy and X-ray diffraction showed that hydrogen bonding between proteins and polysaccharides promoted polymer structure formation after electrostatic interaction and improved compatibility. Thermal stability evaluation revealed that the thermal stability of the blended fibers was superior to that of PUL powder and PUL fibers. The MFGM/PUL nanofibers significantly improved the survival rate of LGG when stored at 4 and 25 °C for 28 days. This study opens up new avenues for food-grade materials in the field of electrostatic spinning and also provides new strategy to effectively protect probiotics.

CRediT authorship contribution statement

Yucong Wang: Methodology, Investigation, Formal analysis, Data curation, Conceptualization. **Zhixin Xie:** Writing – review & editing, Writing – original draft, Validation, Conceptualization. **Haitian Li:** Visualization, Validation, Software, Methodology. **Gongsheng Zhang:** Methodology. **Rongxu Liu:** Validation, Software, Conceptualization. **Jianchun Han:** Writing – review & editing, Supervision, Resources, Project administration, Funding acquisition, Conceptualization. **Lili Zhang:** Writing – review & editing, Supervision, Resources, Project administration, Funding acquisition, Conceptualization.

Declaration of competing interest

The authors declare that they have no known competing financial interests or personal relationships that could have appeared to influence the work reported in this paper.

Data availability

The data that has been used is confidential.

Acknowledgements

The fund Heilongjiang Provincial Key R&D Project (GZ20230023) is correct. A new fund is added : Ruikangyuan Ltd. Co. (ref. sky20200921).

References

Aceituno-Medina, M., Lopez-Rubio, A., Mendoza, S., & Lagaron, J. M. (2013). Development of novel ultrathin structures based in amaranth (Amaranthus hypochondriacus) protein isolate through electrospinning. *Food Hydrocolloids, 31*(2), 289–298. https://doi.org/10.1016/j.foodhyd.2012.11.009

Adesulu-Dahunsi, A. T., Jeyaram, K., & Sanni, A. I. (2018). Probiotic and technological properties of exopolysaccharide producing lactic acid bacteria isolated from cereal-based nigerian fermented food products. *Food Control, 92*, 225–231. https://doi.org/10.1016/j.foodcont.2018.04.062

Alehosseini, A., Sarabi-Jamab, M., Ghorani, B., & Kadkhodaee, R. (2019). Electro-encapsulation of Lactobacillus casei in high-resistant capsules of whey protein containing transglutaminase enzyme. *LWT, 102*, 150–158. https://doi.org/10.1016/j.lwt.2018.12.022

Ali, K., Jiang, B., Chen, J., Ashraf, W., & Tahir, A. B. (2023). Preparation and structural characterization of pullulan and whey protein isolate-based electrospun nanofiber. *Food Bioscience, 56*, Article 103218. https://doi.org/10.1016/j.fbio.2023.103218

Ashwar, B. A., Gani, A., Gani, A., Shah, A., & Masoodi, F. A. (2018). Production of RS4 from rice starch and its utilization as an encapsulating agent for targeted delivery of probiotics. *Food Chemistry, 239*, 287–294. https://doi.org/10.1016/j.foodchem.2017.06.110

Chang, X., Lambo, M. T., Liu, D., & Li, X. (2021). The study of the potential application of nanofiber microcapsules loading lactobacillus in targeted delivery of digestive tract in vitro. *LWT, 148*, Article 111692. https://doi.org/10.1016/j.lwt.2021.111692

Chen, T., Liu, H., Deng, C., Zhou, C., & Hong, P. (2022). Optimization and characterization of the gelatin/wheat gliadin nanofiber electrospinning process. *Food Biophysics, 17*(4), 621–634. https://doi.org/10.1007/s11483-022-09748-5

Cherbut, C., Turini Marco, E., Corthesy-Theulaz, I., Rochat, F., Bergonzelli, G., & Garcia-Rodenas Clara, L. (2004). *NUTRITIONAL FORMULA FOR OPTIMAL GUT BARRIER FUNCTION*. NESTEC SA.

Chou, L.-S., & Weimer, B. (1999). Isolation and characterization of acid- and bile-tolerant isolates from strains of Lactobacillus acidophilus1. *Journal of Dairy Science, 82*(1), 23–31. https://doi.org/10.3168/jds.S0022-0302(99)75204-5

Colín-Orozco, J., Zapata-Torres, M., Rodríguez-Gattorno, G., & Pedroza-Islas, R. (2015). Properties of poly (ethylene oxide)/ whey protein isolate nanofibers prepared by electrospinning. *Food Biophysics, 10*(2), 134–144. https://doi.org/10.1007/s11483-014-9372-1

Drosou, C., Krokida, M., & Biliaderis, C. G. (2018). Composite pullulan-whey protein nanofibers made by electrospinning: Impact of process parameters on fiber morphology and physical properties. *Food Hydrocolloids, 77*, 726–735. https://doi.org/10.1016/j.foodhyd.2017.11.014

Ebadi Nezhad, S. J., Edalatian Dovom, M. R., Habibi Najafi, M. B., Yavarmanesh, M., & Mayo, B. (2020). Technological characteristics of Lactobacillus spp. isolated from Iranian raw milk Motal cheese. *LWT, 133*, Article 110070. https://doi.org/10.1016/j.lwt.2020.110070

Farhang, B., Kakuda, Y., & Corredig, M. (2012). Encapsulation of ascorbic acid in liposomes prepared with milk fat globule membrane-derived phospholipids. *Dairy Science & Technology, 92*(4), 353–366. https://doi.org/10.1007/s13594-012-0072-7

Frakolaki, G., Giannou, V., & Tzia, C. (2023). Encapsulation of Bifidobacterium animalis subsp. lactis through emulsification coupled with external gelation for the development of Synbiotic systems. *Probiotics and Antimicrobial Proteins, 15*(5), 1424–1435. https://doi.org/10.1007/s12602-022-09993-7

Fung, W.-Y., Yuen, K.-H., & Liong, M.-T. (2011). Agrowaste-based nanofibers as a probiotic Encapsulant: Fabrication and characterization. *Journal of Agricultural and Food Chemistry, 59*(15), 8140–8147. https://doi.org/10.1021/jf2009342

Gallier, S., Tolenaars, L., & Prosser, C. (2020). Whole goat Milk as a source of fat and Milk fat globule membrane in infant Formula. *Nutrients, 12*(11). https://doi.org/10.3390/nu12113486

Guerin, J., Burgain, J., Gomand, F., Scher, J., & Gaiani, C. (2019). Milk fat globule membrane glycoproteins: Valuable ingredients for lactic acid bacteria encapsulation? *Critical Reviews in Food Science and Nutrition, 59*(4), 639–651. https://doi.org/10.1080/10408398.2017.1386158

Haghi, A. K., & Akbari, M. (2007). Trends in electrospinning of natural nanofibers. *Physica Status Solidi, 204*(6), 1830–1834. https://doi.org/10.1002/pssa.200675301

Jia, X.w., Qin, Z.y., Xu, J.x., Kong, B.h., Liu, Q., & Wang, H. (2020). Preparation and characterization of pea protein isolate-pullulan blend electrospun nanofiber films. *International Journal of Biological Macromolecules, 157*, 641–647. https://doi.org/10.1016/j.ijbiomac.2019.11.216

Jia, Y.-T., Gong, J., Gu, X.-H., Kim, H.-Y., Dong, J., & Shen, X.-Y. (2007). Fabrication and characterization of poly (vinyl alcohol)/chitosan blend nanofibers produced by electrospinning method. *Carbohydrate Polymers, 67*(3), 403–409. https://doi.org/10.1016/j.carbpol.2006.06.010

John, J. V., McCarthy, A., Su, Y., Ackerman, D. N., Shahriar, S. M. S., Carlson, M. A., & Xie, J. (2022). Nanofiber capsules for minimally invasive sampling of biological specimens from gastrointestinal tract. *Acta Biomaterialia, 146*, 211–221. https://doi.org/10.1016/j.actbio.2022.04.045

Joye, I. J., & McClements, D. J. (2014). Biopolymer-based nanoparticles and microparticles: Fabrication, characterization, and application. *Current Opinion in Colloid & Interface Science, 19*(5), 417–427. https://doi.org/10.1016/j.cocis.2014.07.002

Karim, M. R., Lee, H. W., Kim, R., Ji, B. C., Cho, J. W., Son, T. W., & Yeum, J. H. (2009). Preparation and characterization of electrospun pullulan/montmorillonite nanofiber mats in aqueous solution. *Carbohydrate Polymers, 78*(2), 336–342. https://doi.org/10.1016/j.carbpol.2009.04.024

Kriegel, C., Arrechi, A., Kit, K., McClements, D. J., & Weiss, J. (2008). Fabrication, functionalization, and application of electrospun biopolymer nanofibers. *Critical Reviews in Food Science and Nutrition, 48*(8), 775–797. https://doi.org/10.1080/10408390802241325

Li, Q., Liang, W., Lv, L., Fang, Z., Xu, D., & Liu, Y. (2024). Preparation of PCL/lecithin/bacteriocin CAMT6 antimicrobial and antioxidant nanofiber films using emulsion electrospinning: Characteristics and application in chilled salmon preservation. *Food Research International, 175*, Article 113747. https://doi.org/10.1016/j.foodres.2023.113747

Li, X., Peng, Y., Li, Z., Christensen, B., Heckmann, A. B., & Hernell, O. (2019). Feeding infants Formula with probiotics or Milk fat globule membrane: A double-blind. *Randomized Controlled Trial. Front Pediatr, 7*, 347. https://doi.org/10.3389/fped.2019.00347

Librán, C. M., Castro, S., & Lagaron, J. M. (2017). Encapsulation by electrospray coating atomization of probiotic strains. *Innovative Food Science & Emerging Technologies, 39*, 216–222. https://doi.org/10.1016/j.ifset.2016.12.013

Liu, Z., Jiang, Z., Zhou, K., Li, P., Liu, G., & Zhang, B. (2007). Screening of bifidobacteria with acquired tolerance to human gastrointestinal tract. *Anaerobe, 13*(5), 215–219. https://doi.org/10.1016/j.anaerobe.2007.05.002

Lopez, C. (2011). Milk fat globules enveloped by their biological membrane: Unique colloidal assemblies with a specific composition and structure. *Current Opinion in Colloid & Interface Science, 16*(5), 391–404. https://doi.org/10.1016/j.cocis.2011.05.007

López-Rubio, A., Sanchez, E., Sanz, Y., & Lagaron, J. M. (2009). Encapsulation of living Bifidobacteria in ultrathin PVOH electrospun fibers. *Biomacromolecules, 10*(10), 2823–2829. https://doi.org/10.1021/bm900660b

Luo, X., Fan, S., He, Z., Ni, F., Liu, C., Huang, M., & Xie, H. (2022). Preparation of alginate-whey protein isolate and alginate-pectin-whey protein isolate composites for protection and delivery of Lactobacillus plantarum. *Food Research International, 161*, Article 111794. https://doi.org/10.1016/j.foodres.2022.111794

Ma, J., Xu, C., Yu, H., Feng, Z., Yu, W., Gu, L., & Hou, J. (2021). Electro-encapsulation of probiotics in gum Arabic-pullulan blend nanofibres using electrospinning technology. *Food Hydrocolloids, 111*, Article 106381. https://doi.org/10.1016/j.foodhyd.2020.106381

Martín, M. J., Lara-Villoslada, F., Ruiz, M. A., & Morales, M. E. (2015). Microencapsulation of bacteria: A review of different technologies and their impact on the probiotic effects. *Innovative Food Science & Emerging Technologies, 27*, 15–25. https://doi.org/10.1016/j.ifset.2014.09.010

Minekus, M., Alminger, M., Alvito, P., Ballance, S., Bohn, T., Bourlieu, C., & Brodkorb, A. (2014). A standardised static in vitro digestion method suitable for food – An international consensus. *Food & Function, 5*(6), 1113–1124. https://doi.org/10.1039/C3FO60702J

Mojaveri, S. J., Hosseini, S. F., & Gharsallaoui, A. (2020). Viability improvement of Bifidobacterium animalis Bb12 by encapsulation in chitosan/poly(vinyl alcohol) hybrid electrospun fiber mats. *Carbohydrate Polymers, 241*, Article 116278. https://doi.org/10.1016/j.carbpol.2020.116278

Paéz, R., Lavari, L., Vinderola, G., Audero, G., Cuatrin, A., Zaritzky, N., & Reinheimer, J. (2012). Effect of heat treatment and spray drying on lactobacilli viability and resistance to simulated gastrointestinal digestion. *Food Research International, 48*(2), 748–754. https://doi.org/10.1016/j.foodres.2012.06.018

Qin, Z.-y., Jia, X.-W., Liu, Q., Kong, B.-h., & Wang, H. (2019). Fast dissolving oral films for drug delivery prepared from chitosan/pullulan electrospinning nanofibers. *International Journal of Biological Macromolecules, 137*, 224–231. https://doi.org/10.1016/j.ijbiomac.2019.06.224

Qin, Z., Jia, X., Liu, Q., Kong, B., & Wang, H. (2020). Enhancing physical properties of chitosan/pullulan electrospinning nanofibers via green crosslinking strategies. *Carbohydrate Polymers, 247*, 116734. https://doi.org/10.1016/j.carbpol.2020.116734

Salminen, S., Collado, M. C., Endo, A., Hill, C., Lebeer, S., Quigley, E. M. M., & Vinderola, G. (2021). The international scientific Association of Probiotics and Prebiotics (ISAPP) consensus statement on the definition and scope of postbiotics. *Nature Reviews Gastroenterology & Hepatology, 18*(9), 649–667. https://doi.org/10.1038/s41575-021-00440-6

Tiwari, S. K., & Venkatraman, S. S. (2012). Importance of viscosity parameters in electrospinning: Of monolithic and core–shell fibers. *Materials Science and Engineering: C, 32*(5), 1037–1042. https://doi.org/10.1016/j.msec.2012.02.019

Wang, Y., Guo, Z., Qian, Y., Zhang, Z., Lyu, L., Wang, Y., & Ye, F. (2019). Study on the electrospinning of gelatin/pullulan composite nanofibers. *Polymers, 11*.

Wu, Y., Wang, K., Liu, Q., Liu, X., Mou, B., Lai, O.-M., & Cheong, L.-Z. (2022). Selective antibacterial activities and storage stability of curcumin-loaded nanoliposomes prepared from bovine milk phospholipid and cholesterol. *Food Chemistry, 367*, Article 130700. https://doi.org/10.1016/j.foodchem.2021.130700

Xiao, Q., & Lim, L.-T. (2018). Pullulan-alginate fibers produced using free surface electrospinning. *International Journal of Biological Macromolecules, 112*, 809–817. https://doi.org/10.1016/j.ijbiomac.2018.02.005

Xu, C., Ban, Q., Wang, W., Hou, J., & Jiang, Z. (2022). Novel nano-encapsulated probiotic agents: Encapsulate materials, delivery, and encapsulation systems. *Journal of Controlled Release, 349*, 184–205. https://doi.org/10.1016/j.jconrel.2022.06.061

Xu, C., Ma, J., Wang, W., Liu, Z., Gu, L., & Jiang, Z. (2022). Preparation of pectin-based nanofibers encapsulating Lactobacillus rhamnosus 1.0320 by electrospinning. *Food Hydrocolloids, 124*, Article 107216. https://doi.org/10.1016/j.foodhyd.2021.107216

Yao, D., Ranadheera, C. S., Shen, C., Wei, W., & Cheong, L.-Z. Milk fat globule membrane: composition, production and its potential as encapsulant for bioactives and probiotics. *Critical Reviews in Food Science and Nutrition*, 1–16. doi:https://doi.org/10.1080/10408398.2023.2249992.

Yilmaz, M. T., Taylan, O., Karakas, C. Y., & Dertli, E. (2020). An alternative way to encapsulate probiotics within electrospun alginate nanofibers as monitored under simulated gastrointestinal conditions and in kefir. *Carbohydrate Polymers, 244*, Article 116447. https://doi.org/10.1016/j.carbpol.2020.116447

Zaeim, D., Sarabi-Jamab, M., Ghorani, B., Kadkhodaee, R., & Tromp, R. H. (2018). Electrospray-assisted drying of live probiotics in acacia gum microparticles matrix. *Carbohydrate Polymers, 183*, 183–191. https://doi.org/10.1016/j.carbpol.2017.12.001

Zhang, G., He, M., Xiao, L., Jiao, Y., Han, J., & Zhang, L. (2024). Milk fat globule membrane protects Bifidobacterium longum ssp. infantis ATCC 15697 against bile stress by modifying global transcriptional responses. *Journal of Dairy Science, 107*(1), 91–104. https://doi.org/10.3168/jds.2023-23591

Zhang, L., Chichlowski, M., Gross, G., Holle, M. J., Lbarra-Sánchez, L. A., & Miller, M. J. (2020). Milk fat globule membrane protects Lactobacillus rhamnosus GG from bile stress by regulating exopolysaccharide production and biofilm formation. *Journal of Agricultural and Food Chemistry, 68*(24), 6646–6655. https://doi.org/10.1021/acs.jafc.0c02267